International Journal of Engineering Research & Technology (IJERT)
ISSN: 2278-0181
Vol. 4 Issue 04, April-2015

Dynamics and Equilibrium Studies of the Adsorption of Cu(II) from Aqueous Solutions by Activated Hibiscus sabdariffa. L. Stalk Biomass

D. L. Ajifack
Lanochee,
Department of Chemistry, Faculty of Science,
University of Dschang,
Cameroon

J. N. Ghogomu
Lanochee,
Department of Chemistry,
Faculty of Science, University of Dschang,
Cameroon

J. N. Ndi
Lptc,
Department of Inorganic Chemistry,
Faculty of Science, University of Yaounde I,
Cameroon

J. M. Ketcha
Lptc,
Department of Inorganic Chemistry,
Faculty of Science, University of Yaounde I,
Cameroon

***Abstract*— The valorization of activated carbon from stalks of *Hibiscus sabdariffa.* L. obtained by chemical activation using [H_3PO_4 (PAAC) and KOH (PHAC)] followed by pyrolysis in the removal of copper from aqueous solution is reported. Samples were characterized by FTIR, XRD, SEM, Boehm method and pH_{ZPC}, macronutrient content and the iodine number determination. Batch adsorption experiments were performed to study the effects of various parameters such as solution pH, contact time, carbonization temperature, initial adsorbate concentration and adsorbent mass at 27 ^{o}C. Analysis of macronutrient content of the *Hibiscus sabdariffa.* L. stalk yielded percentages of fixed carbon, moisture content, ash content and volatile matter equal to 70.36%, 3.90%, 6.28%, 19.46% respectively. Optimal conditions from equilibrium studies for the adsorption of copper(II) ions were as follows: contact times of 30 and 40 minutes for PAAC and PHAC respectively, pH=4.5 for both samples, adsorption capacities of 81.5mg/g for PAAC and 90.5 mg/g for PHAC. Adsorption isotherms were described by Langmuir, Freundlich and Temkin isotherm models. Equilibrium data were best represented by Langmuir isotherm model with monolayer adsorption capacities of 100.0 mg/g and 76.92 mg/g for PAAC and PHAC respectively. Kinetic studies revealed that adsorption rates followed pseudo-second order model. *Hibiscus sabdariffa.* L. stalks based activated carbons (HSSBAC) is shown to be a promising material for the adsorption of copper(II) ions from aqueous solutions.**

Keywords*—Hibiscus sabdariffa. L. stalks, chemical activation, activated carbon, adsorption of Cu(II)

I. INTRODUCTION

Today water pollution constitutes a major environmental challenge (quality of life) due to the release of toxic heavy metals, hydrocarbons, dyes, etc. from various industries. Solutions to this general problem encompass the notion of time and type of pollutants discharged. These heavy metals are not biodegradable and their presence in streams and lakes leads to bioaccumulation in living organisms causing health problems in animals, plants, and human beings [1]. Copper is essential to life and health but, like all heavy metals, it is potentially toxic as well. Its accumulation have been reported in the liver, brain, pancreas and myocardium of humans that often lead to Wilson Disease [2]. Continued inhalation of copper-containing spray is linked with an increase in lung cancer among exposed workers.

As a result of these, environmental regulatory boards often spell out limitations as to the maximum concentration of copper in natural water bodies and for wastewater discharge. Copper is used in cloth making, marine painting, electrical equipments, boilers, pipes, etc. International norms according to WHO prescribe limiting concentrations of Copper in drinking water to 1 mg/L of copper [3].

The development of several techniques such as chemical precipitation, adsorption on mineral or organic materials, emulsified liquid membranes and membrane processes (microfiltration, ultrafiltration, nanofiltration, reverse osmosis, ion-exchange resins), complexation, adsorption, solvent extraction, distillation [4], are geared towards greater amelioration of the quality of the environment/water quality. Amongst these methods, adsorption which is reported in this work has shown high potentials and simplicity in management in the depollution of industrial waste water, especially in the elimination of some heavy metals [5]. Nevertheless, its efficacy depends largely on the adsorbent (cost, availability, and its regeneration) put in place. The cost of preparing activated carbon from agricultural wastes is negligible when compared to the cost of commercial activated carbon [6]. Several researchers have envisaged the use of alternative materials, which, although at time less efficient, involve lower costs (see Table I): [7] prepared hazelnut shell-based activated carbon for the sorption of Cu(II) ions in aqueous solution with a high specific surface area and a maximum adsorption capacity of about 3.07mg/g of Cu(II) from a model based on the Langmuir adsorption isotherm. According to [8], maximum adsorption of Cu(II) ions by $ZnCl_2$ activated carbon prepared from rice husk was of the order of 112.43 mg/g of adsorbent. On their own part, [9] investigated on the adsorption performance of *Cynodon Dactylon*-based

activated carbon for the uptake of Cu(II) and reported a monolayer adsorption capacity of 117.51 mg/g via the same model. In the same vein, this study has been to evaluate the ability of chemically activated carbon prepared from low-cost *Hibiscus sabdariffa* L. stalks by phosphoric acid and potassium hydroxide for the adsorption of Cu(II) from aqueous solutions.

TABLE I. COMPARISON OF ADSORPTION CAPACITY OF COPPER (II) WITH OTHER ADSORBENTS

Adsorbents	Qm (mg/g)	References
hazelnut shells	3.07	[7]
Rice Husk	112.43	[8]
Cynodon Dactylon	117.51	[9]
PAAC	100.0	Present Study
PHAC	76.92	Present Study

II. MATERIALS AND METHODS

A. Sources and preparation of adsorbents

All the reagents and chemicals used were of A.R grade (Merck, Labtech). The working solutions were prepared in distilled water. Stems of roselle (*Hibiscus sabdariffa*.L) from the *sabdariffa* variety were collected from a farm land at the locality of the City of Santchou located in the Western Region of Cameroon and were abundantly washed with distilled water to eliminate the impurities, and then dried under open air for 7 days. The washed and dried raw material underwent coarse crushing in order to obtain homogeneous materials. After sieving through standard steel sieves, only fractions with diameters ranging between 0.5 and 1.25 mm were retained.

B. Chemical Activation and Pyrolysis

In this study, chemical activation was achieved by using phosphoric acid (H_3PO_4) and potassium hydroxide (KOH) as activation agents. The precursor material obtained was of diameters ranging between (0.50-1.25 mm) as indicated above. The method involved mixing the chosen precursor fraction of *Hibiscus sabdariffa*. L. stalks with either 10% wt of H_3PO_4 (for PAAC samples) or 50% wt of KOH (for PHAC samples) before carbonization. 30.0 g of dried *Hibiscus sabdariffa*. L. stalks were impregnated with solutions of activating agent (KOH or H_3PO_4) in a desired weight ratio of *Hibiscus sabdariffa*. L. stalks to the activating agent of 1:1. Each mixture was left for 30 min at room temperature. The impregnated samples were placed in an oven at 110°C for 24 hours. Pyrolysis of the impregnated samples was carried-out for one hour duration in a carbolite furnace in the absence of air (oxygen) which was preheated to an initial room temperature (25-27°C) and then to a final temperature of 400, 500, and 600°C at a heating rate of 10 °C min^{-1} for 1 hour duration (activation time), which was then allowed to cool down to ambient temperature, after which a dry residue was obtained. Total elimination of phosphate ions from the PAAC samples were achieved by abundant washing with distilled water until a neutral pH was obtained. On their part, PHAC samples were initially washed abundantly with a 10% solution of hydrochloric acid followed by abundant washing with distilled water until the pH of the resulting samples ranged from 6-7 in order to eliminate all chloride ions [10]. The resultant activated carbon samples (PAAC and PHAC) were then oven-dried at 110°C for a period of 24 hours. The final material samples were ground and then sieved to obtain particles with diameters less than 71 microns.

III. CHARACTERIZATION OF ADSORBENT

A. Proximate analysis

Proximate analysis determined by the standard test method ASTM D2866-94 [11], was used to determine the macronutrient in the *Hibiscus sabdariffa*. L. stalk waste when the sample was heated and treated under specific conditions.

B. Moisture content

Thermal drying method was used in the determination of moisture content of the samples. For this test, 5.0 g of the precursor were weighed in triplicates and placed in washed, dried and weighed crucibles. The crucibles were heated at 110 °C to constant weight for 24 hours in an oven. The weight of the samples before and after heating was determined in order to calculate the amount of moisture in the sample. The percentage moisture content was computed as follows:

$$\text{Moisture content (\%)} = \frac{\text{Loss in weight on drying (g)}}{\text{Initial sample weight (g)}} \times 100 \quad (1)$$

C. Ash content

The standard test method for ash content-ASTM D2866-94 was used. To determine the ash content, dried sample of activated carbon weighed to the nearest 1.0 g was taken into the crucible (of known weight). The crucible was placed in the carbolite furnace and heated to 600 ^oC and ashing was considered to be completed when constant weight is achieved. The crucible was cooled to room temperature in a desiccator and the percentage weight of the remaining sample was considered as ash content. The ash content was calculated using (2).

$$\text{Ash content (\%)} = \frac{\text{Ash weight (g)}}{\text{Oven dry weight (g)}} \times 100 \quad (2)$$

D. Volatile matter and fixed carbon content of samples

Approximately 1.0 g of sample was put into a crucible with lid and of known weight. The crucible with content was then placed inside a carbolite furnace regulated at 600 ^oC for 1 hour. After cooling the crucible to room temperature in a desiccator, its weight was recorded. The percentage weight loss was regarded as the percentage of volatile matter and calculated according to (3);

$$\text{Volatile matter (\%)} = \frac{\text{Weight of volatile component (g)}}{\text{Oven dry weight (g)}} \times 100 \quad (3)$$

Fixed carbon content of the samples was obtained from the moisture, ash and volatile matter contents as follows:

$$\text{Fixed carbon (\%)} = 100\% - \text{moisture (\%)} + \text{volatile matter (\%)} \quad (4)$$

E. Iodine number (I_n)

The iodine number was measured according to the procedure established by the American Society for Testing and Materials (ASTM D2866-94) [11]. It is the number of milligrams of iodine adsorbed by 1.0 g of carbon when the iodine concentration of the filtrate is 0.02 N. The iodine number is accepted as the most fundamental parameter used to characterize activated carbon performance. Iodine number was employed in this study as a test for microporosity

via volumetric analysis. This fundamental test for the potentials of the prepared activated carbon determines its microporosity up to values as small as 2 nm. The iodine number is obtained from the following expression:

$$\text{Iodine number} = \frac{(25.4\times(30-V_n))}{m_{AC}} \quad (5)$$

Where, m_{AC} (g) is the mass of the activated carbon and V_n (mL), the volume of the sodium thiosulphate solution at the equivalence point.

F. *Standardization of iodine solution*

10 mL of 0.02 N iodine solutions were measured into a conical flask and 2-3 drops of starch solution added to it. The pale yellow color of the iodine solution turned blue and was titrated with a 0.005 N sodium thiosulphate until it became colorless.

G. *Surface function determination by the Boehm method*

Titration of the total surface acidity and basicity of the activated carbons was carried out via the Boehm method [12]. In the determination of acidic surface functions (carboxylic, lactonic, phenolic), 40 mL each of decimolar solutions of $NaHCO_3$, Na_2CO_3, NaOH and HCl, were introduced into different reactors and each put in contact with 0.1 g of activated carbon sample. Titration of excess base was done by HCl solution. In the determination of the basic functions, 0.1 g of activated carbon was put in contact with 40 mL of a decimolar solution of HCl. After stirring for 48 hours, the excess acid was titrated with NaOH.

H. *Determination of pH at zero-point charge (pHzpc)*

pH of zero charge, pHzpc, corresponds to a pH at which the surface charge is nul. pHzpc of the activated carbon samples were estimated according to standard procedure [13]. 50.0 mL of a decimolar solution of NaCl was introduced into reactors each containing 0.1 g of activated carbon to be analyzed. The pH of each solution was adjusted by addition of decimolar solutions of NaOH or HCl (by varying values of pH between 3 and 11). pHzpc was determined by the intersection of the representative curves pH (final) = f[pH (initial)] and the first bisector curve. Stirring was maintained at 27 °C for 48 hours with the aid of a multi-agitator system (Edmund Bühler GmbH) 150 rpm. The contents of the reactors were then filtered with Whatman N°4 filter paper after which the pH of the final solutions was measured.

I. *Analysis by Fourier-transform-IR spectrophotometer (FTIR)*

In order to determine the surface functional groups existing on the carbon samples, FTIR were carried out on samples using infrared spectrophotometer (Brüker alpha–p spectrometer) with ethanol as solvent with a resolution of 4cm^{-1} within the interval 400-4000 cm^{-1}.

J. *Scanning Electron Microscopy (SEM) analyses*

In a bid to study the surface morphology and to verify the porosity of the adsorbents, the prepared activated carbon samples were examined by Scanning Electron Microscope (SEM' PHILIPS XL30 S-FEG) equipped with a spectrometer having a cathode luminescence detector. These were obtained by the juxtaposition of SEM images of our precursor samples with those of the carbonized PAAC and PHAC. The precursor and the activated carbon samples from each preparation method that had high iodine number were chosen for SEM analysis.

K. *Powder X-ray diffraction (PXRD) study*

XRD patterns of *Hibiscus sabdariffa*. L. samples were recorded on a Phillips PW1450/70 diffractometer equipped with a PW1390 channel control goniometer supply, argon filled proportional counter used as a detector was linked to a PW1373 rate meter and channel analyzer. CuKα =0.15418 nm radiation was generated using a Phillips PW1730 X-ray generator operated at 40 kV and 30 mA. Powdered samples were pressed into pellets on a hydraulic press (25 kN) before XRD measurements.

IV. BATCH ADSORPTION EXPERIMENTS

A. *Preparation and determination of Cu(II) Ion solution*

The mother solution was prepared by dissolving 8.04834 g of $CuCl_2.2H_2O$ (M=170.48 g/mol at 99% purity by mass, Merck, Germany) inside a 1-Liter volumetric flask with freshly prepared distilled water and completing to the mark after agitation for 1 hour. Successive dilution of mother solution gave rise to the working solutions.

B. *Equilibrium Studies Using Batch Method*

Kinetic and equilibrium studies of Cu(II) ion adsorption were carried out in a thermostatic batch reactor maintained at 27 °C. In each triplicate trial, 0.1 g of carbon sample preserved as described above was weighed and introduced into 20.0 mL of a Cu(II) ion solution contained in a beaker. pH of the resultant solutions was adjusted by addition of 0.1 N solution of HCl or NaOH to a pre-determined value. This procedure didn't concern those involving the influence of pH. The effect of adsorbent dose was determined at an initial metal ion concentration of 2400 ppm and at pH 4.5 and varying adsorbent dosage from 0.1 g to 0.5 g. The effect of pH on the adsorption of Cu(II) ions was investigated while varying the pH as described above between 2 and 4.5. In kinetic studies, the different mixtures obtained were stirred within a time interval of 5-60 minutes for equilibrium time determination. The residual Cu(II) ion concentration in each sample, after filtration of the residual solutions with Whatman filter paper N°4 was determined by UV- visible spectrophotometer (CORNING 259) at 830 nm wavelength. The sorption capacity of samples at equilibrium (Qe) and the percentage removal (% R) are given by (6) and (7) below:

$$Q_e = \frac{(C_0 - C_e)V}{m} \quad (6)$$

$$\%R = \frac{C_0 - C_e}{C_0}\times 100 \quad (7)$$

V. RESULTS AND DISCUSSION

A. *Characterization of Adsorbents*

The knowledge of the characteristics of the activated carbon is necessary to contribute to the comprehension of many phenomena like adsorption, desorption, or others.

B. *Proximate analysis*

Fig. 1 (results of approximate chemical analysis) indicates that this material is characterized by an ash content of 6.28% which is within the norms (<10%): the lower the ash content, the better the activated carbon samples will be; a moisture content of 3.90% which is also within the norms (<5%) since the traditional value of the water content varies between 1 to 5% by mass [14]. This figure also shows a low volatile matter of 19.46% and high fixed carbon content of 70.36%. This justifies our choice of *Hibiscus sabdariffa*. L. as an excellent low-cost precursor in the production of activated carbon.

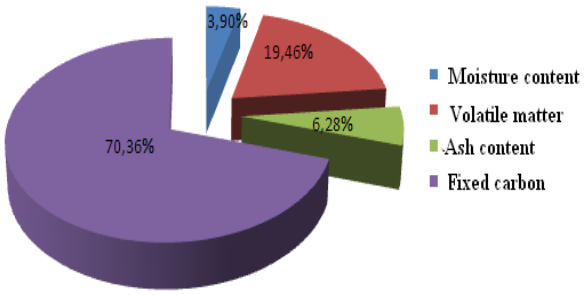

Fig. 1. The proximate analysis giving composition of *Hibiscus sabdariffa*. L

C. *Effect of temperature on the iodine number*

Carbonization temperature is one of the most influential of the factors that govern porosity development during the activation process [15]. When phosphoric acid activated roselle (*Hibiscus sabdariffa*. L) is subjected to high temperature, phosphorus compounds are liberated at its surface because of its lignocellulosic nature [16]. Fig. 2 shows a reversed effect of the carbonization temperature on the iodine index of the samples between 400 °C and 600 °C. Any temperature increase results in a decrease in the microporosity of the activated carbon samples and consequently a sharp decrease in their adsorption capacity. Iodine index reached maximum values for these studies at 400 °C both for PAAC and PHAC. Similar results and conclusions were arrived at by [17].

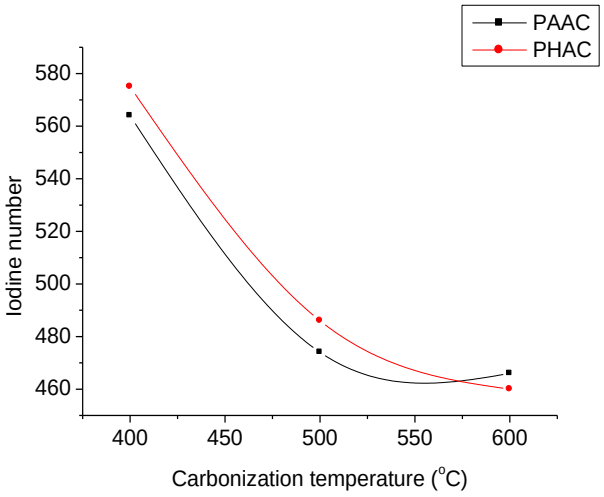

Fig. 2. Effect of carbonization temperature on the iodine number.

D. *Powdered X – Ray Diffraction Spectroscopy (PXRD)*

Fig. 3 below shows the profile of the X-ray diffraction of the stems of the inactivated *Hibiscus sabdariffa*.L prepared under optimal conditions. Analyses were carried out at angles ranging between 10° and 70°. We notice on the profile that the raw material presents a peak at approximately 24°, which could be due to the presence of certain chemical substances assimilated by the *Hibiscus sabdariffa*. L plant from the soil during its growth. After carbonization this peak disappears and the two activated carbon samples present broader peaks with the absence of pointed peak that essentially reveals the primarily amorphous structure, which is an advantageous property indicative of the porous structure of the carbon samples, PAAC and PHAC [18]. We also notice that the lines of diffraction are badly formed or very broad, which is indicative of low crystallinity or even of an amorphous structure [19]. The broad peak found at approximately 24° for the two carbons confirm that the samples are nongraphited, and can have a high microporous structure [20].

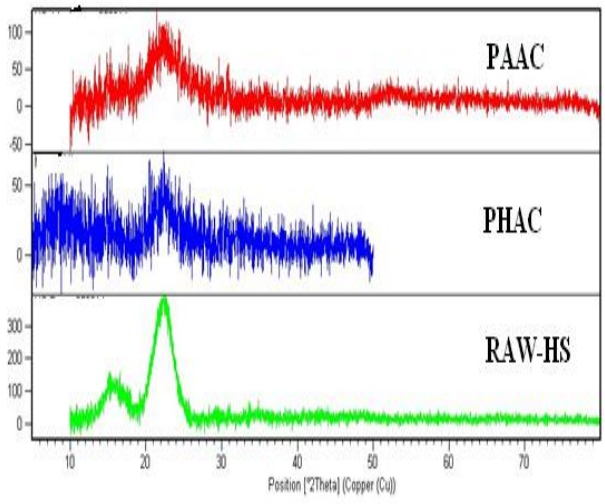

Fig. 3. X-ray diffraction of the *Hibiscus sabdariffa.* L.

E. Determination of Oxygen Containing Functional Groups

On Table 2 is presented the results of the quantification of the surface acidic and basic functions of the activated carbon samples (PAAC and PHAC) obtained via the Boehm method. Chemical analysis of the surface revealed that both samples contain more acidic (carboxylic and phenolic groups) than basic functions with a diminishing lactonic group. This observation is in conformity with the pH_{PZC} values which are in proportions with the acidic and basic functions.

F. Determination of pH at zero-point charge (pHzpc)

The pHzpc obtained for each activated carbon (Fig. 4) is coherent with the quantification of the surface functional groups obtained via the Boehm method. These pHzpc values permit the determination of the acidic or basic character of the activated carbon and to know, according to the pH of the solution, the net surface charge. According to Fig. 4, it can be noticed that pHzpc=6.0 for PAAC and that pHzpc=5.2 for PHAC. Hence, in experiments wherein pHzpc >pH samples will have their surfaces positively charged while for those in which pHzpc <pH will have their surfaces negatively charged. This result is of great importance on the interactions between the molecules and the adsorbent in the liquid phase.

TABLE II. QUANTIFICATION OF SURFACE OXYGEN-CONTAINING GROUPS BY THE BOEHM METHOD

Activated carbon	Carboxylic (meq g^{-1})	Lactonic (meq g^{-1})	Phenolic (meq g^{-1})	Total acid (meq g^{-1})	Total basic (meq g^{-1})	Total (meq.g^{-1})
PAAC	0.254	0.001	0.077	0.296	0.167	0.463
PHAC	0.254	0.000	0.073	0.294	0.125	0.419

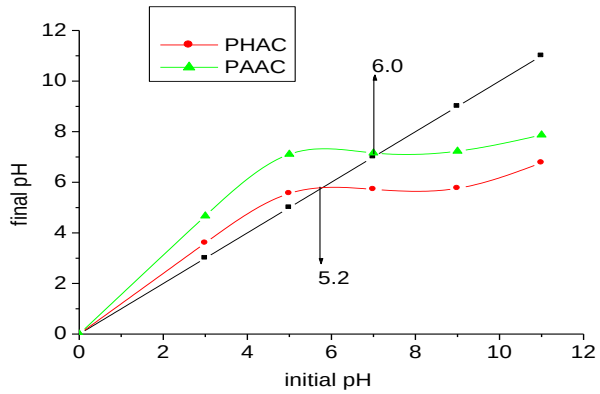

Fig. 4. Graph for the determination of pHzpc for PAAC and PHAC

G. Fourier Transform Infrared spectroscopy (FTIR)

The analysis of the Fourier-Transform Infra-Red spectrum of the activated carbon (PAAC and PHAC) enabled us to identify the major chromophores responsible for the various signals respectively (Fig. 5 and 6; tables 3 and 4).

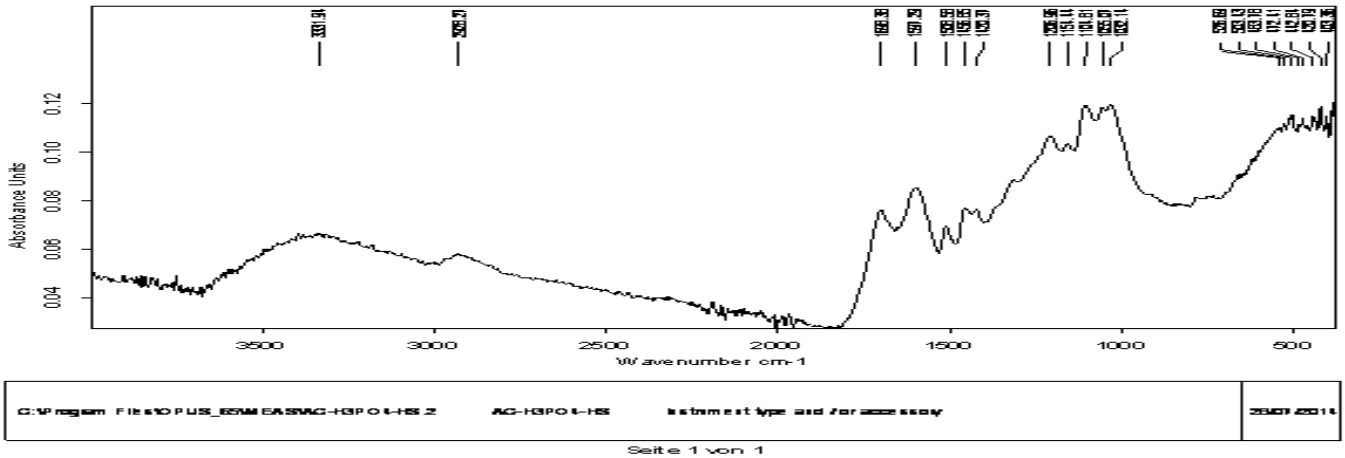

Fig. 5. FTIR of *Hibiscus sabdariffa*. L. stalks based for PAAC

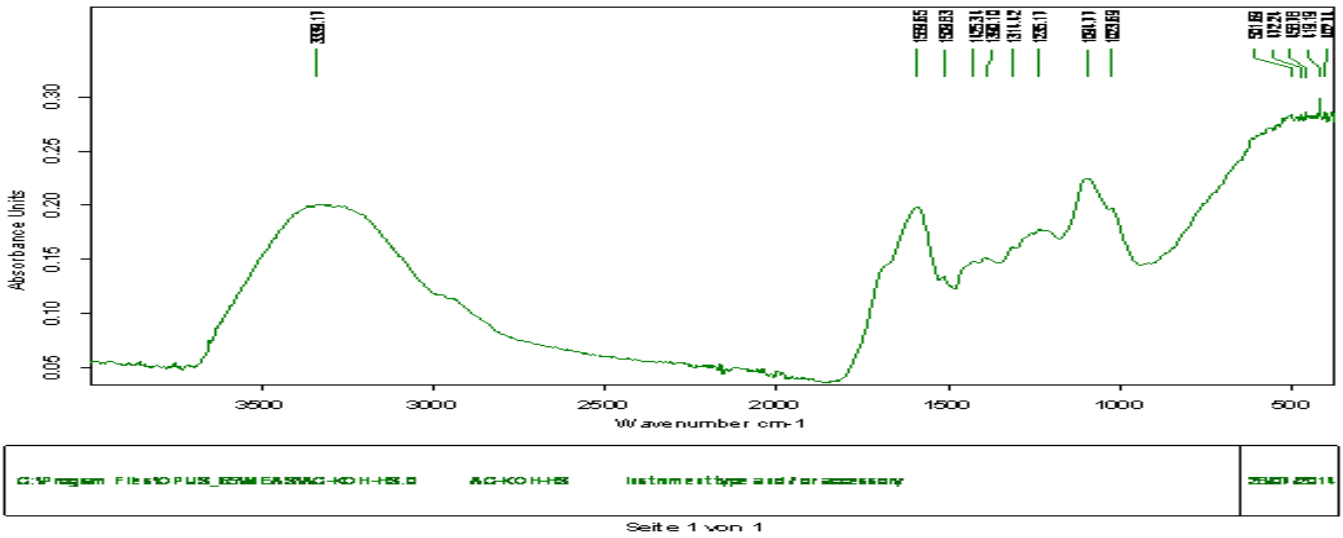

Fig. 6. FTIR of *Hibiscus sabdariffa*. L. stalks based for PHAC

TABLE III. INTERPRETATION OF THE IR SPECTRUM OF PAAC (FIG. 5)

Absorption bands (cm^{-1})	Chromophores and functional groups
3600-3000	OH of carboxylic, phenols, alcohols, water
2928	CH of aromatic methoxyl groups
1698	C=O of ketones, aldehydes, lactones or of the carboxylic groups
1597	C=C bonds in the aromatic cycles
1456-1420	CH2 and/or O-H of carboxylic and phenol groups
1206 and 1032	C-O is characteristic of phosphorus and phosphorus-carbonated compounds of the phosphoric acid activated carbon [21].
526- 403	Para distribution of the aromatic cycles [22].

TABLE IV. INTERPRETATION OF THE IR SPECTRUM OF PHAC (FIG. 6)

Absorption bands (cm^{-1})	**Chromophores and functional groups**
3339	OH of carboxylic, phenols, alcohols, water
1589	C=C stretching variation in aromatic boxing rings
1425-1390	C-OH stretching vibration in carboxylic group
1314 – 1235	C-O stretching vibration in phenol and alcohol groups
1094-1023	C-O-C asymmetrical stretching
501-402	Para distribution of the aromatic cycles [22].

H. Scanning Electron Microscopy (SEM)

SEM micrographies of the precursor and the chemically activated carbons by H_3PO_4 and KOH respectively (PAAC and PHAC) are presented on Fig 7.We notice here that the precursor has a surface with no visible pores. The effect of chemical activation is observable on the micrography of PAAC and PHAC as they show well developed porosities (regarded as channels with microporous network). These adsorbents (PAAC and PHAC) have rough textures, heterogeneous surfaces and random pore size distribution. The existence of macro fractures and the presence of a multitude of fine particles attached to the activated carbon [23] is noticeable. These particles are visible on the micrographies and attributed to impurities acquired during the preparation but also a reminiscence of the vegetable origin of carbon.

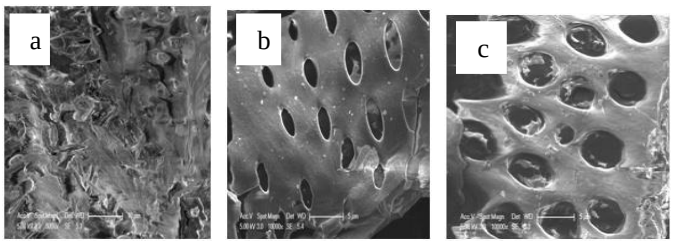

Fig. 7. Morphology of samples: a) precursor b) PHAC et c) PAAC

I. Effect of contact time

Contact time is inevitably a fundamental parameter in all transfer phenomena including adsorption. The effect of contact time on Cu(II) adsorption capacity is illustrated in Fig. 8. In this experiment carried out at pH =4.5, adsorption rate initially increased rapidly and attained maximum for both samples (81.5mg/g for PAAC and 90.5 mg/g for PHAC) after equilibrium times of 40 and 30 minutes for PAAC and PHAC respectively . There was no significant change in equilibrium concentration after these periods. It is evident from this study that, Cu (II) uptake is rapid at the initial stage of contact time and slowly increases at higher contact time until saturation. This is explained by the fact that initially there is available free space for adsorption and after some time, the remaining vacant surface sites become difficult to be occupied due to repulsive

forces between the adsorbate molecules on the solid surface and in the bulk phase. Thus, the driving force for the mass transfer between the bulk liquid phase and the solid phase decreases with time. Furthermore, the metal ions have to traverse farther distance and move deeper into the pores encountering much larger resistance. This results in the slowing down of the adsorption during the later phase [24].

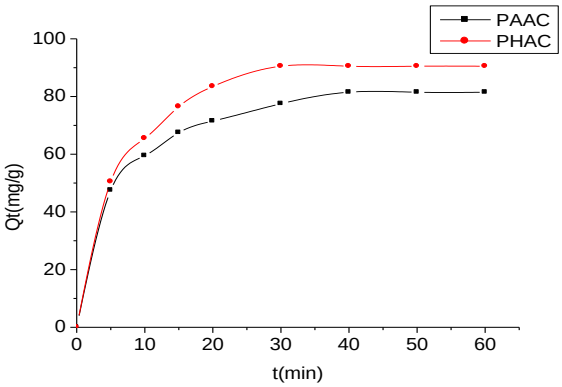

Fig. 8. Effect of contact time on copper (II) adsorption for PAAC and PHAC (adsorbent dose=0.1g, pH=4.5, T= 27 °C).

J. *Effect of initial pH*

pH is an important controlling parameter in aqueous adsorption process as it influences the surface charge of adsorbents and the nature of the ionic species of the adsorbates. The experiments were done under different pH values (between 2.0 and 4.5) keeping other parameters constant. The experimental results are presented in Fig. 9. By increasing pH, increase in adsorption capacity was observed and the maximum adsorption capacity of copper was obtained at pH 4.5 corresponding to 81.5mg/g and 90.5mg/g (PAAC et PHAC respectively. Continual increase in pH lead to a decrease in adsorption percentage attributed to the precipitation of $Cu(OH)_2$. This might also be due to the weakening of electrostatic force of attraction between the oppositely charged adsorbate and adsorbent that ultimately lead to the reduction in sorption capacity.

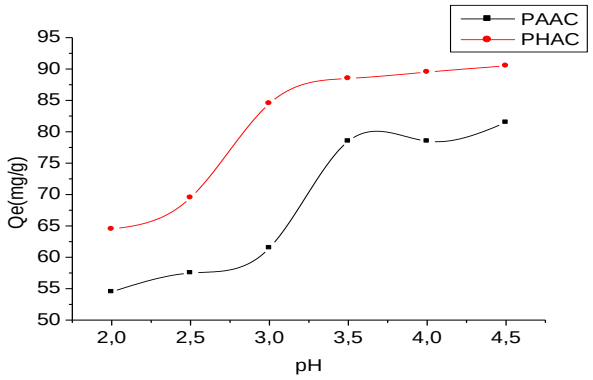

Fig. 9. Effect of initial pH on copper (II) adsorption onto PAAC and PHAC (C=2400ppm, adsorbent dose=0.1g, t= 40min for PAAC and t=30 min for PHAC, T= 27 °C).

K. *Effect of adsorbent dose*

The effect of adsorbent dose was determined at an initial metal ion concentration of 2400 ppm and at pH 4.5. The results summarized in Fig. 10 indicate that, with an increase in adsorbent dose, adsorption capacity rapidly decreases within the range 0.1- 0.5 g. This effect can be due to some adsorption sites remaining unsaturated during the adsorption process. Low Cu(II) removal as adsorbent dose increased may be due to the fact that the adsorption of Cu(II) is limited by monolayer adsorption. This is corroborated by the value of the correlation coefficient, R^2, from Langmuir isotherm [25].

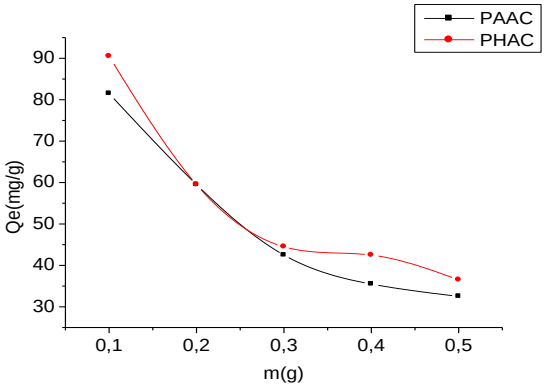

Fig. 10. Effect of adsorbent dose on copper(II) adsorption for PAAC and PHAC (C=2400ppm, pH=4.5, t= 40min for PAAC and t=30 min for PHAC, T= 27 °C).

L. *Effect of initial concentration of copper*

Studies were performed with Cu(II) initial concentrations ranging from 0.9 to 2.4g/L. An amount of 0.1 g of adsorbent with pH 4.5 was used for adsorption experiment. The experimental results of the effect of initial copper(II) concentration on the adsorption capacity are presented in Fig. 11. It is obvious from this figure that, Cu(II) adsorption increases with increase in initial Cu(II) concentration. This is because an increases in the initial concentration of Cu(II) ions brings about an increase in mass transfer from the aqueous phase to the solid phase. However, at higher copper concentrations, the available adsorption sites become fewer, and hence the adsorption of Cu(II) becomes more or less constant.

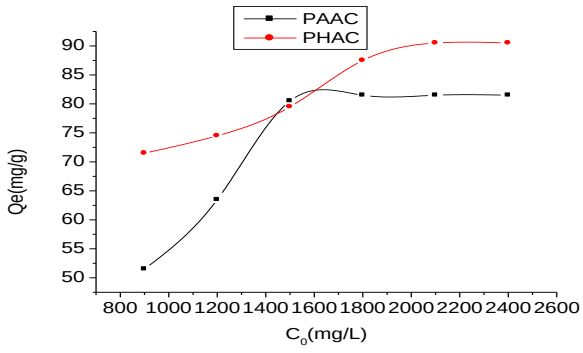

Fig. 11. Effect of initial concentration on copper (II) adsorption for PAAC and PHAC (adsorbent dose=0.1 g, pH=4.5, t= 40min for PAAC and t=30 min for PHAC, T= 27 °C).

M. Sorption Kinetic Models

Several kinetic models are often used in modeling the adsorption mechanism of dissolved solutes on adsorbents. In this study, four kinetic models have been studied in describing the adsorption phenomenon of Cu (II) ions onto the two activated carbon samples studied herein: pseudo-first order, pseudo-second order, Elovich and intra-particle diffusion models.

N. Pseudo first-order

In order to study the adsorption kinetics of Cu(II) ions, the kinetics parameters for the adsorption process were studied for contact times ranging from 5 to 60 min by monitoring the quantity of Cu(II) adsorbed as a function of time. The data were then regressed against the Lagergren equation (8), which represents a first order kinetics equation [26].

$$\ln(Q_e - Q_t) = \ln Q_e - K_1 t \quad (8)$$

where, k_1 is the pseudo-first-order rate constant (min^{-1}); Q_e and Q_t are the adsorption capacities at equilibrium and at a given time t expressed in (mg/g).

O. Pseudo second-order model

Represented by (9) below, the linearized pseudo-second order chemisorption kinetic model [10, 27] has been frequently used in diverse experiments involving the adsorption of organics and heavy metals on activated carbon.

$$\frac{t}{Q_t} = \frac{1}{K_2 Q_e^2} + \frac{t}{Q_e} \quad (9)$$

Where, K_2 is the pseudo-second-order rate constant ($mg.g^{-1}.min^{-1}$).

P. Elovich model

The linearized Elovich equation is generally expressed as:

$$Q_t = \frac{1}{\beta}\ln(\alpha\beta) + \frac{1}{\beta}\ln(t) \quad (10)$$

Where, α is the initial sorption rate (mg g^{-1} min) and β is the desorption rate constant (g mg^{-1}) during any one experiment and by assuming that $\alpha\beta t >> 1$[28].

Q. Intra-particle diffusion model

During the batch mode of operation, there is a possibility of transport of sorbate species into the pores of the sorbent, which is often the rate controlling step. The rate constants of intra particle diffusion (K_{id}) at different copper ion concentrations were determined using the following linearized equation

$$Q_t = K_{id} t^{1/2} + C \quad (11)$$

Where Q_t is the amount of Cu(II) sorbed at time t and $t^{1/2}$ is the square root of the time. K_{id} is the intra-particle diffusion constant ($mg.g\text{-}1.min^{-1/2}$). When intra-particle diffusion plays a significant role in controlling the kinetics of the sorption process, straight line plots through the origin are obtained and their slopes give the rate constant, k_{id}.

The slopes and intercepts of all the model curves were used to determine values of the constants as well as the equilibrium capacity (Qe). The results indicate that the adsorption process follows only the second-order kinetic rate equation after fitting the adsorption data of Cu(II) ions onto the two activated carbon samples (Fig. 12) with correlation factors R^2 = 0.999 and 0.998 for PAAC and PHAC respectively. This implies that adsorption of copper (II) ions onto both adsorbents may occur through a chemical process involving the valence forces of the shared or exchanged electrons [29]. This means that chemisorption reaction or an activated process becomes more predominant in the rate-controlling step for the copper system. The straight-line plot for second order rate equation has been represented on (Fig. 12) and the values of all the model parameters and the correlation coefficients are presented in Table 5. The fact that linear plots for intraparticle diffusion model for each sample did not pass through the origin is indicative that the intraparticle diffusion was not a rate controlling step.

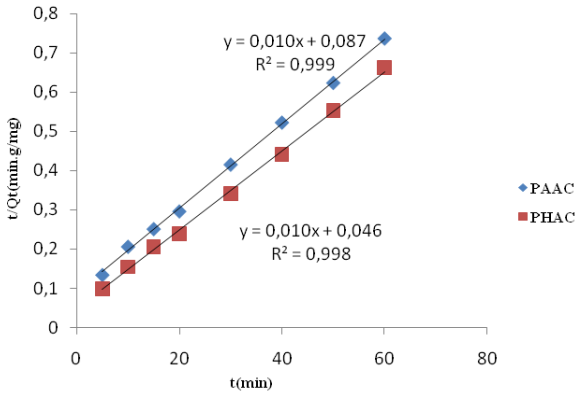

Fig. 12. Linearized pseudo- second order plots for Co=2400mg/L, V=20mL, pH=4.5, m=0.1g adsorbent.

TABLE V. RESULTS OF ADSORPTION PARAMETERS FOR THE DIFFERENT KINETIC MODELS

Models	Parameters	Adsorbents	
		PAAC	*PHAC*
Pseudo-first order	R^2	0.869	0.700
	K_1 (min^{-1})	0.001	0.001
Pseudo-second Order	R^2	0.999	0.998
	h (mg/g. min)	11.49	21.73
	K_2 ($x10^{-3}$g/mg. min)	1.149	2.173
	Qe (mg/g)	100.0	100.0
Elovich	R^2	0.948	0.915
	β (g/mg)	0.056	0.056
	α (mg/g min) $x10^{-9}$	3.367	68.39
Intra-particle Diffusion	R^2	0.878	0.794
	Kid (min^{-1})	5.970	6.824
	a (mg/g)	40.90	45.34

R. Adsorption isotherm models

The distribution of adsorbate between the liquid phase and the solid phase, notably, the degree of accumulation of adsorbate on the surface of the adsorbent, the solute-solution interaction, and knowledge of the adsorption capacity of the adsorbent can be described by several isotherm models such as Langmuir, Freundlich and Temkin models [30].

S. Langmuir adsorption isotherm

The Langmuir model assumes that the uptake of metal ions occurs on a homogeneous surface by monolayer adsorption without any interaction between adsorbed ions, that uniform energies of adsorption are involved, and that there is no transmigration of adsorbate in the plane of the surface [31]. The linearized Langmuir isotherm equation can be expressed as:

$$\frac{C_e}{Q_e} = \frac{K_L}{Q_m} + \frac{C_e}{Q_m} \qquad (12)$$

Where, K_L is the Langmuir adsorption constant (L/mg) which is related to the maximum sorption capacity and energy of adsorption, Ce is the equilibrium concentration (mg/L), Qe is the amount adsorbed per amount of adsorbent at equilibrium (mg/g) and Qm (mg/g) is an indicator of monolayer adsorption capacity. The efficiency of the Langmuir adsorption process is further assessed by (13):

$$R_L = \frac{1}{1 + K_L C_0} \qquad (13)$$

Where R_L is a dimensionless constant referred to as separation factor, K_L is the Langmuir constant related to the energy of adsorption and C_0 is the initial solute concentration (mg/L). If $R_L > 1$ adsorption is said to be unfavorable, $R_L = 1$ for linear adsorption, $0 < R_L < 1$ for favorable adsorption and $R_L = 0$ for irreversible adsorption.

T. Freundlich adsorption Isotherm

The Freundlich model assumes that the uptake of metal ions occurs on a heterogeneous surface by monolayer adsorption [32]. The linearized relation (14) is given below:

$$\ln Q_e = \ln K_F + \frac{1}{n} \ln C_e \qquad (14)$$

Where: Q_e is the quantity of solute adsorbed at equilibrium (adsorption density: mg of adsorbate per g of adsorbent). Ce is the concentration of adsorbate at equilibrium, $1/n$ (mg/L) is the adsorption intensity or the heterogeneity factor and K_F is the Freundlich constant related to the adsorption energy (mol^2/kJ^2). These last two constants are dependent of temperature and the nature of sorbent and sorbate.

U. Temkin adsorption isotherm.

It is expressed in linear form by the following relationship between the amount adsorbed, Q_e, and concentration in solution at equilibrium, C_e, [33]:

$$Q_e = B_T (\ln A_T + \ln C_e) \qquad (15)$$

Where, A_T (L/g) is the Temkin isotherm constant (equilibrium binding constant), B_T (J/mol) is a constant related to heat of sorption, R is the gas constant (8.314 $Jmol^{-1}$. K^{-1}) and T is the absolute temperature (K). Similar to the Freundlich equation, the Temkin model takes into account the heterogeneity of the surface [33].

In order to find the most appropriate model for the copper adsorption, the data were fitted to each isotherm model. The parameters of the different models are presented on Table 5 and only the Langmuir isotherm model (R^2= 0.995 and 0.997 for PAAC and PHAC respectively) represented on Fig. 13 [34] best fitted the experimental data. The homogeneous monolayer adsorption capacity of Cu(II) ions at 27 °C were found to be equal to 100.0 mg/g and 76.92 mg/g for PAAC and PHAC samples respectively. The shape of the Langmuir isotherm was investigated by the dimensionless constant separation term (R_L). In this investigation the equilibrium parameter was found to be in the range $0 < RL < 1$ as shown in Table 6. This indicated that the sorption process was very favorable and that the adsorbent employed exhibits good adsorption potentials. Temkin isotherm model predicts a uniform distribution of binding energies over the population of surface binding adsorption. The values of Temkin constants A_T and B_T as well as the correlation coefficients are listed in Table 6.

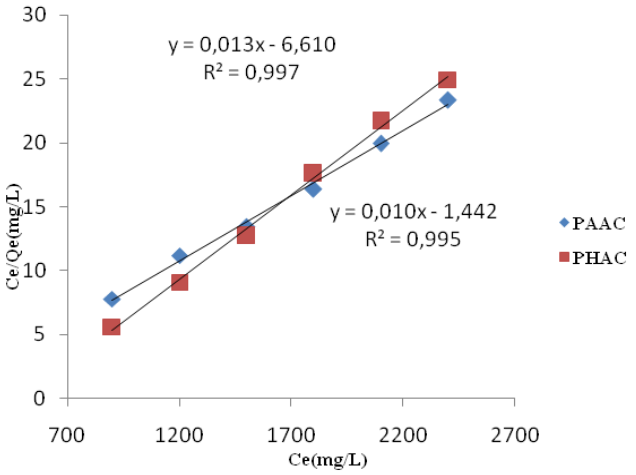

Fig. 13. Linear transformation of Langmuir isotherm

TABLE VI. RESULTS OF ADSORPTION PARAMETERS FOR THE DIFFERENT MODEL ISOTHERMS

Models	Parameters	Adsorbents	
		PAAC	*PHAC*
Langmuir Isotherm	R^2	0.995	0.997
	Qmax (mg/g)	100.0	76.92
	K($x10^{-3}$L/mg)	6.934	1.966
	R_L	(0.138-0.056)	(0.361-0.174)
Freundlich Isotherm	R^2	0,874	0,936
	1/n	0.318	0.169
	K_F(L/g)	7.916	24.95
Temkin isotherm	R^2	0.955	0.964
	A_T (L/g)	1.193	1.078
	B_T (KJ/mol)	0.118	0.183

VI. CONCLUSION

This work shows that by appreciably reducing the temperature of carbonization to 400 °C one obtains higher values of iodine indices for HSSBAC (PAAC and PHAC) with interesting adsorption capacities. The chemical analysis by the Boehm method and the results obtained from FTIR analysis showed the presence of the functional groups on the surface of the activated carbon. Although kinetic data for the Cu(II)

sorption were fitted to four kinetics models, namely the pseudo-first- and pseudo-second-order, intraparticle diffusion and Elovich model, only the pseudo-second-order model, (R^2=0.999 and 0.998) best described the sorption process for both adsorbents (PAAC and PHAC) respectively. The equilibrium sorption of Cu(II) ion by PAAC and PHAC was analyzed by the Langmuir, Freundlich and Temkin isotherm models. The Langmuir isotherm was the most appropriate model with a monolayer sorption capacity of Cu(II) ion of 100.0 mg/g and 76.92 mg/g for PAAC and PHAC respectively working at pH=4.5 at 27°C. The present study shows that the *Hibiscus sabdariffa.* L. stalks based activated carbons (HSSBAC) are effective adsorbents for the sorption of Cu(II) ion by PAAC and PHAC.

ACKNOWLEDGMENT

The author, D.L.A, wishes to express sincere gratitude to the University of Dschang Research Board for the research grants to meritorious post graduate students that took care of the characterization of the prepared activated samples within and without the country.

REFERENCES

[1] S. Ong, C. Seng, and P.Lim, "Kinetics of adsorption of Cu (II) and Cd (II) from aqueous solution on husk and modified rice husk". EJEAFche, vol. 6 (2), pp.1764-1774. 2007.

[2] J. Chen, J. Yoon and S.Yiacoumi, "Effects of chemical and physical properties of influent on copper sorption onto activated carbon fixed-bed columns", Carbon, Vol. 41, pp.1635–1644, 2003;

[3] K.S. Rao, S. Anand and P. Venkateswarlu, "Adsorption of Cadmium(II) Ions from Aqueous Solution by Tectona Grandis (Teak leaves power)", Bioresources, Vol.5, pp.438-454, 2010.

[4] V. K. Gupta, and I. Ali, "Removal of lead and chromium from wastewater using bagasse fly ash-sugar industry waste", J. Colloid Interface Sci, Vol. 271(2), p.321, 2004.

[5] A. A. Ahmad, B.H. Hameed, N. Aziz, "Adsorption of direct dye on palm ash: Kinetic and equilibrium modeling". Journal of Hazardous Materials, pp.1-10, 2006.

[6] Upendrakumar, Agricultural products and by-products as a low cost adsorbent for heavy metal removal from water and wastewater: A review, Sci. Res. and Essay, Vol.1(2), pp.033-037, 2006.

[7] D. M. Dragan, M. Milutin, A. Milosavljević, D. Marinković, R ĐVeljko, Z. M. Jelena and L. B. Aleksandar, "Removal of copper(II) ion from aqueous solution by high-porosity activated carbon", Vol. 39 pp.515-521, 2013.

[8] K. Nasehir, E. M Yahaya, F. P. Muhamad, L. Mohamed, I. Abustan, S. B. Olugbenga, and A. A. Mohd, "Adsorptive Removal of Cu (II) Using Activated Carbon Prepared From Rice Husk by $ZnCl_2$ Activation and Subsequent Gasification with CO_2", International Journal of Engineering & Technology IJET -IJENS Vol. 11(01), pp.164-168, 2011.

[9] U. Gayathri, B.R. Venkatraman, S. Arivol, "Removal of Copper (II) Ions from Aqueous Solutions by Adsorption with Low Cost Acid Activated Cynodon Dactylon Carbon". E-Journal of Chemistry Vol. 8(1), pp. 377-391, 2011.

[10] D. L. Ajifack, J. N. Ghogomu, T. D. Noufame, J. N. Ndi and J. M. Ketcha, "Adsorption of Cu (II) Ions from Aqueous Solution onto Chemically Prepared Activated Carbon from Theobroma cacoa". British Journal of Applied Science & Technology, vol. 4(36), pp.5021-5044, October 2014.

[11] O. A. Ekpete, and M. J. Horsfall, "Preparation and characterization of activated carbon derived from fluted pumpkin stem waste (Telfairiaoccidentalis Hook F)", Res. J. Chem. Sci. vol. 1(3), pp. 10-17, April 2011.

[12] H. Boehm, E. Diehl, W. Heck and R. Sappok, "Surface oxides on carbon, Angew Chemistry", p. 669, 1964.

[13] M. V.Lopes-Ramon, F.Stoeckli , C.Moreno-Castilla and F.Carrasco-Marin, "On the characterization of acidic and basic surface sites on carbons by various techniques", Carbon, vol. 37, pp.1215-1221, 1999.

[14] Z. Belkebir, "Valorisation des déchets agro-alimentaires Cas des grignons d'olives". Mémoire de Magister, université m'Hamed bougara –boumerdes, p.66, 2007.

[15] J.V.Nabais, P.Carrott, M.M. Carrott, V. Luz, and A.L. Ortiz, "Influence of preparation conditions in the textural and chemical properties of activated carbons from a novel biomass precursor: the coffee endocarp". Bioresource Technology, vol. 99, pp.7224-7231, 2008.

[16] M. K Gratuito, T. Panyathanmaporn, R.A. Chumnanklang, N. B Sirinuntawittaya and A. Dutta, "Production of activated carbon from coconut shell: optimization using response surface methodology", 2008.

[17] N.J. Ndi, M. J. Ketcha, G. S. Anagho, N. J. Ghogomu and E. P Belibi, "Physical and chemical characteristics of activated carbon prepared by pyrolysis of chemically treated Cola nut (cola acuminata) Shells wastes and its ability to adsorb organics". International Journal of Advanced Chemical Technology, vol. 3, pp.1-13, 2014.

[18] W.Tongpoothorn, M. Sriuttha, P. Homchan, S. Chanthai, and C. Ruangviriyachai, "Preparation of activated carbon derived from Jatropha curcas fruit shell by simple thermo-chemical activation and characterization of their physic-chemical properties", Chemical Engineering Research and Design, vol. 89, pp. 335-340, 2011.

[19] A. Kriaa, N. Hamdi, and E. Srasta, "Removal of Cu(II) from water Pollutant with Tunisian activated lignin prepared by phosphoric acid activation", Desalination, vol. 250, pp.179-187, 2010.

[20] J. Zhao, L. Yang, F. Li, R. Yu, and C. Jin, "Structural evolution in the graphitization process of activated carbon by high-pressure sintering", Carbon, vol. 47, pp.744-751, 2009.

[21] A. M. Puziy, O. I. Poddubnaya, A. Martinez-Alonso, F. Suarez-Garcia and J. M. Tascon D. "Surface chemistry of phosphorus containing carbons of lignocellulosic origin", Carbon vol. 43(14), pp.2857–2868, 2005.

[22] M. Hesse, H. Meir, B. Zeeh, "Méthodes Spectroscopiques pour la chimie organique", Masson, Paris, 1997.

[23] S. Zeroual, K. Guerfi , S. Hazourli, and C. Charnay. "Estimation de l'hétérogénéité d'un charbon actif oxydé à différentes températures à partir de l'adsorption des molécules sondes", Revue des Energies Renouvelables Vol. 14 (4) pp.581 – 590, 2011.

[24] A. M. Jennifer, "Adsorption of substituted aromatic compounds by actived carbon: A mechanistic approach to quantitative structure activity relationships", *PhD Thesis, University of Florida*, p.71, 2005.

[25] W. Rafeah, N. Zainab, and U. J.Veronica, "Removal of mercury, lead and copper from aqueous solution by activated carbon of palm oil empty fruit bunch World", Applied Sciences Journal (Special Issue for Environment), Vol. 5, pp. 84-91, 2009.

[26] A. Mohammad, A. R. Mohammad, A. M. Mohammad, B. S. Mohammad, "Adsorption Studies on Activated Carbon Derived from Steam Char", Indian Society for Surface Science and Technology, India Vol. 23(1-2): pp. 73-80, 2007.

[27] Ho YS, McKay G. "The kinetic of sorption of divalent metal ions onto sphagnum moss peat", Water Research. 2000; Vol. 34: pp. 735-742.

[28] E. Elkhatib, A. Mahdy, M. Saleh, and N. Barakat "Kinetics of copper desorption from soils as affected by different organic Ligands" Int. J. Environ. Sci. Tech., Vol.4(3), pp. 331-338, 2007.

[29] S.Wang, and H. Li, "Kinetic modelling and mechanism of dye adsorption on unburned carbon". Dyes Pigments, Vol. 72(3), pp. 308-314, 2007.

[30] P. S. Kumar, and K. Kirthika "Equilibrium and kinetic study of adsorption of nickel from aqueous solution onto bael tree leaf powder", J Eng Sci Technol Vol. 4, pp. 351–363, 2009.

[31] A. Jeyaseelan, M. Shanmugaprakash, H. S. Sangeetha, C. Lenin and P. Kanmani "Pigeon pea (Cajanus cajan) pod as a novel eco-friendly biosorbent: a study on equilibrium and kinetics of Ni(II) biosorption", International Journal of Industrial Chemistry, Vol. 4, p. 25, 2013.

[32] J. N. Ndi and M. J. Ketcha, "The Adsorption Efficiency of Chemically Prepared Activated Carbon from Cola Nut Shells by ZnCl2 on Methylene Blue", Journal of Chemistry. Vol. 2013, Article ID 469170, p. 7, 2013.

[33] J. N. Ghogomu, T. D Noufame, M. J Ketcha and N. J. Ndi "Removal of Pb (II) ions from Aqueous Solutions by Kaolinite and Metakaolinite materials", Bristich Journal of Applied Science and Technology, Vol. 3(4): pp. 942-961, 2013.

[34] E. Demirbas, and M.Z. Nas, "Batch kinetic and equilibrium studies of adsorption of Reactive Blue 21 by fly ash and sepiolite", Desalination, Vol. 243(1-3), pp. 8-21, 2009.